Spin rectification induced by spin Hall magnetoresistance at room temperature

Cite as: Appl. Phys. Lett. **109**, 112406 (2016); https://doi.org/10.1063/1.4962895
Submitted: 23 June 2016 . Accepted: 31 August 2016 . Published Online: 16 September 2016

P. Wang, S. W. Jiang, Z. Z. Luan, L. F. Zhou, H. F. Ding, Y. Zhou, X. D. Tao, and D. Wu

Spin rectification induced by spin Hall magnetoresistance at room temperature

P. Wang, S. W. Jiang, Z. Z. Luan, L. F. Zhou, H. F. Ding,[a] Y. Zhou, X. D. Tao, and D. Wu[a]
National Laboratory of Solid State Microstructures, Department of Physics and Collaborative Innovation Center of Advanced Microstructures, Nanjing University, 22 Hankou Road, Nanjing 210093, People's Republic of China

(Received 23 June 2016; accepted 31 August 2016; published online 16 September 2016)

We have experimentally and theoretically investigated the dc voltage generation in the heterostructure of Pt and yttrium iron garnet under the ferromagnetic resonance. Besides a symmetric Lorenz line shape dc voltage, an antisymmetric Lorenz line shape dc voltage is observed in field scan, which can solely originate from the spin rectification effect due to the spin Hall magnetoresistance. The angular dependence of the dc voltage is theoretically analyzed by taking into account both the spin pumping and the spin rectification effects. We find that the experimental results are in excellent agreement with the theoretical model, further identifying the spin Hall magnetoresistance origin of the spin rectification effect. Moreover, the spin pumping and the spin rectification effects are quantitatively separated by their different angular dependence at particular experimental geometry. *Published by AIP Publishing*. [http://dx.doi.org/10.1063/1.4962895]

There has been rapidly growing interest in the study of pure spin currents without charge currents due to their promise for high efficiency and low power consumption electronic devices.[1] Spin pumping effect (SPE) is one of the widely used approaches to generate a pure spin current and was initially demonstrated in metallic multilayers.[2,3] The precession of spin driven by the ferromagnetic resonance (FMR) emits a pure spin current from a ferromagnet into an adjacent normal metal (NM). The spin current is then converted to a dc voltage in the NM layer by means of the inverse spin Hall effect (ISHE). In addition to the spin-pumping dc voltage (V_{SP}), the spin precession can simultaneously rectify the microwave current into a dc voltage via the anisotropic magnetoresistance (AMR) and/or the anomalous Hall effect (AHE) of the ferromagnetic metal.[4–7] These two effects are superimposed. They can be precisely separated and identified by their different symmetries.[8] V_{SP} has only a symmetric line shape with respect to the ferromagnetic resonance field H_r, whereas the spin-rectification dc voltage (V_{SR}) has both symmetric and antisymmetric line shapes. Moreover, V_{SP} and V_{SR} have different symmetries with respect to the angle between the field and the measurement direction.[9,10]

In a heterostructure of the NM and ferrimagnetic insulator (FI), the spin precession of the FI can produce V_{SP} in the adjacent NM layer by the SPE and ISHE, similar to the metallic multilayer system.[11,12] For the spin rectification effect (SRE), it is expected to be absent because of no free electrons and hence AMR and AHE effects in the FI. However, recent studies on NM/FI heterostructures discovered a new type of magnetoresistance (MR), named the spin Hall magnetoresistance (SMR).[12–14] Although the physical mechanism of SMR such as the magnetic proximity effect (MPE) and the concerted actions of the spin Hall effect (SHE) and ISHE is still intensively debated,[13,15] SMR is robust and has been observed in several different systems.[16,17] SMR analogue to AMR is anisotropic, i.e., the resistance of the NM layer dependent on the magnetization **M** direction of the FI. Therefore, it was proposed in theory that the SRE can also occur to produce a dc voltage via SMR in the NM/FI bilayer.[18] Owing to SMR about two orders of magnitude smaller than AMR, V_{SR} is expected to be small and negligible. A clear evidence of the existence of the SMR-induced SRE has not been provided in experiments.[18,19]

In this letter, we experimentally demonstrated that a dc rectification voltage can be generated by the magnetization dynamics coming from SMR under FMR in the Pt/$Y_3Fe_5O_{12}$ (YIG) system. The SRE is identified by the antisymmetric Lorenz line shape dc voltage in field scan, similar to the AMR-induced SRE.[8] The symmetric Lorenz line shape dc voltage is the superposition of V_{SP} and SMR-induced V_{SR}. We present a model to calculate V_{SR} induced by SMR with respect to the applied magnetic field **H** and the microwave field **h**. The measured data can be well explained by the model, evidencing the presence of the SMR-induced SRE. We found that the contributions of V_{SP} and V_{SR} to the symmetric dc voltage can be quantitatively separated by the field angular dependence measurements at particular experimental geometry.

YIG films were epitaxially grown on $Gd_3Ga_5O_{12}$ (GGG) (111) substrates using pulsed laser deposition by applying a KrF excimer laser at a repetition of 4 Hz and a laser fluence of $\sim$2.7 J/cm^2. The growth temperature and oxygen pressure were 730 °C and 0.05 Torr, respectively. Clear *in situ* reflection high-energy electron diffraction (RHEED) patterns were observed during deposition, indicating the single crystallinity of the YIG films. The film quality was further confirmed by X-ray diffraction. The magnetic properties of YIG were characterized by a vibrating sample magnetometer (see supplementary material). The YIG films were transferred into another vacuum chamber to deposit 5-nm-thick Pt films by dc magnetron sputtering, of which the resistivity is 3.03×10^{-5} Ω·cm. The Pt films were

[a]Electronic addresses: hfding@nju.edu.cn and dwu@nju.edu.cn

defined to be a 4-mm-long and 0.1-mm-wide Hall bar by shadow masks for the magnetoresistance (MR) measurements, which were measured by a Keithley 2002 voltmeter in a four-wire mode in a Quantum Design physical property measurement system (PPMS).

The coordinate system in all the measurements is defined in Fig. 1(a), in which the dc or rf current is along the x-axis. α, β, and γ are the angles between **H** and x-, y-, and z-axes, respectively. Figure 1(b) shows the resistance R as a function of **H** for the Pt (5 nm)/YIG (20 nm)/GGG (111) bilayer measured by a four-probe method at room temperature with **H** applied along the dc current direction and perpendicular to the current. MR is clearly present. The angular dependence of MR is a key to distinguish between SMR and AMR.[13] For the angle-dependent measurements, R was monitored with rotating the samples in a constant magnetic field in the xy- (α-scan), yz- (β-scan), and xz- (γ-scan) planes, respectively. The results obtained in different geometries with $H = 3000$ Oe are shown in Fig. 1(c). For α-scan (top panel), **H** is strong enough to align **M** along **H** due to the weak magneto-crystal anisotropy in YIG. The MR ratio, defined as $\Delta R/R = [R(\text{angle}) - R(\text{angle} = 90°)]/R(\text{angle} = 90°)$, can be well described by a $\cos^2\alpha$ function. For β-scan (middle panel), **H** and **M** are non-collinear due to the demagnetization field, even though **H** is larger than the saturation field of ~1800 Oe. ψ_M, the angle between **M** and z-axis, can be calculated by taking the demagnetization field into account: $2H\sin(\beta - \psi_M) + 4\pi M_s \sin 2\psi_M = 0$, where M_S is the saturation magnetization of YIG. Then, we found that the MR ratio can be well described by a $\cos^2\psi_M$ function (see supplementary material). For γ-scan (bottom panel), MR disappears. These behaviors are the characteristics of SMR and in agreement with previous reports,[12,13] suggesting that SMR is observed in our Pt/YIG samples. In addition to SMR, there is an extra MR at large field. However, MR should remain constant above saturation field for both AMR and SMR. This extra MR has been attributed to MPE and the Hanle effect-induced MR.[20,21] H_r of YIG in SRE measurements is less than 3000 Oe (see supplementary material). This extra MR ratio is estimated to be less than 0.001% for $H = 3000$ Oe, more than one order of magnitude smaller than the SMR ratio. Therefore, we do not consider this extra MR in the SRE.

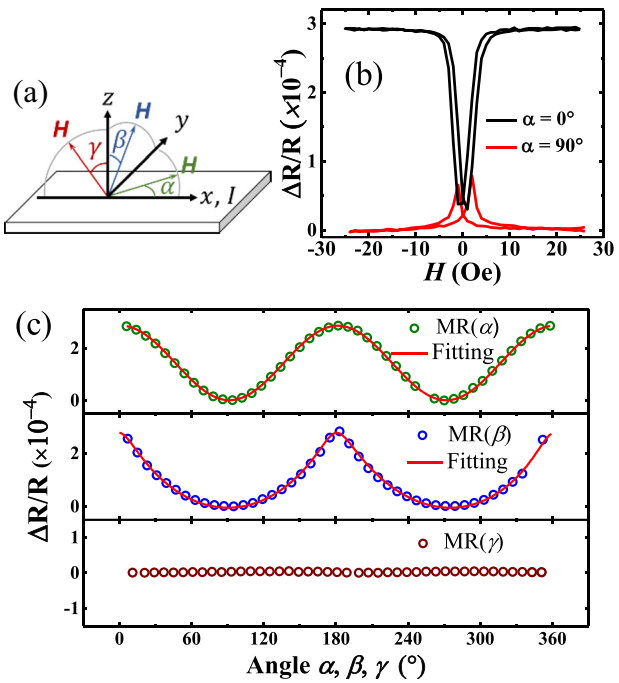

FIG. 1. (a) Spatial coordinates of the measurements, where the current is along the x-axis. (b) MR of the YIG (20 nm)/Pt (5 nm) bilayer for $\alpha = 0°$ and $\alpha = 90°$. (c) MR as functions of the magnetic field directions with $H = 3000$ Oe. The red curves are fitting lines according to the SMR theory.

For the SPE and SRE measurements, the samples were placed upside down in the center of the signal line of a coplane waveguide (CPW) and electrically isolated from CPW by a polymer solder resist layer, as sketched in Fig. 2(a). The CPW comprises a 1-mm-wide signal line and 0.2-mm-wide gaps between the signal line and ground lines. The dc voltage $V(H)$ is measured along the x-direction. A microwave signal of about 100 mW power was inputted into the CPW in all measurements. We used a Stanford SR830 lock-in amplifier to pick up the dc voltage signal and the microwave signal was modulated at 11.73 kHz. All the experiments were performed at room temperature.

Figure 2(b) shows $V(H)$ of the Pt/YIG bilayer while **H** is applied within the film plane with $\alpha = 45°$ at a microwave frequency $f = 3$ GHz. The line shape of $V(H)$ is clearly not symmetric with respect to H_r. Since the spin-pumping signal only gives a symmetric line shape,[2,22] the measured $V(H)$ is not solely contributed from the SPE. We found that $V(H)$ can be well described by a supercomposition of a symmetric Lorenz curve and an antisymmetric Lorenz curve, $V(H) = V_S\text{Sym}(H) + V_A\text{Asym}(H) + V_C$, where $\text{Sym}(H) = \Delta H^2/[(H - H_r)^2 + \Delta H^2]$ represents the Lorenz function, V_S is the amplitude of the Lorentz line shape, ΔH is the half width at half maximum, $\text{Asym}(H) = \Delta H(H - H_r)/[(H - H_r)^2 + \Delta H^2]$ represents the antisymmetric Lorenz function, V_A is the amplitude of the antisymmetric line shape, and V_C is a constant value. V_C is

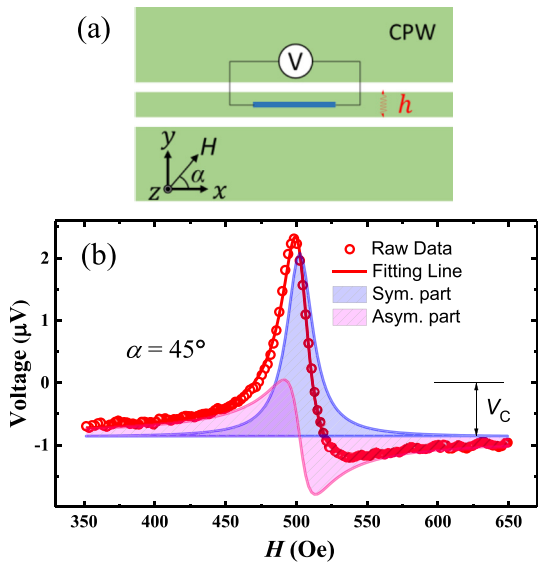

FIG. 2. (a) Sketch of the experimental set-up. The YIG/Pt bilayer was placed upside down along the signal line of the CPW with **h** mainly along the y-axis. (b) The dc voltage (open circles) was detected by sweeping H at $\alpha = 45°$. The red fitting line is given by a superposition of symmetric (blue) and antisymmetric (pink) components after removing a constant value V_C, originated from the spin Seebeck effect.

attributed to the spin Seebeck effect and it will be discussed below. We attributed the observed antisymmetric signal to the SMR-induced SRE.

In the following, we further analyzed the angular dependence of $V(H)$ to confirm the SRE. In spherical coordinates $(\mathbf{e}_r, \mathbf{e}_\theta, \mathbf{e}_\phi)$, as shown in Fig. 3(a), the precession motion of $\mathbf{M}$ driven by the microwave magnetic field $\mathbf{h}(t) = (h_\theta \mathbf{e}_\theta + h_\phi \mathbf{e}_\phi)\exp(i\omega t)$ can be described by $\mathbf{m}(t) = \mathbf{M}/M = \mathbf{m}_0 + (m_\theta \mathbf{e}_\theta + m_\phi \mathbf{e}_\phi)\exp(i\omega t)$, where $\mathbf{m}_0$ is the equilibrium magnetization direction along $\mathbf{e}_r$. The induced microwave current $I(t) = I_1 \exp(i\omega t + \delta)$, where δ is the phase between the rf current and the rf magnetic field, flowing along the x-direction and through the Pt film produces a voltage $V(t) = (R - R_S m_y^2(t))I(t)$, where R_S is the SMR-related resistance change. This is the origin of the SMR-induced SRE. Here, the y-component of $\mathbf{m}(t)$, $m_y(t)$, in Cartesian coordinates $(\mathbf{e}_x, \mathbf{e}_y, \mathbf{e}_z)$, shown in Fig. 3(a), is given by $m_y(t) = \sin\psi_M(t)\sin\varphi_M(t)$, where φ_M is the angle between the xy-plane projection of $\mathbf{M}$ and x-axis. By using $\psi_M(t) = \theta_M + \theta_1(t)$ and $\varphi_M(t) = \phi_M + \phi_1(t)$ where θ_M is the angle of $\mathbf{m}_0$ with respect to the z-direction and ϕ_M is the angle between the xy-plane projection of $\mathbf{m}_0$ and x-axis and considering that the magnetization precession angle $\theta_1(t)$ and $\phi_1(t)$ are very small, we obtain an ac voltage as

$$V(t) \cong R_S I(t)[\sin(2\theta_M)\sin^2(\phi_M)\theta_1(t) + \sin(2\phi_M)\sin^2(\theta_M)\phi_1(t)]. \quad (1)$$

By using $\theta_1(t) \approx m_\theta \exp(i\omega t)$ and $\phi_1(t) \approx m_\phi \exp(i\omega t)/\sin\theta$ and expressing m_θ and m_ϕ in terms of h_θ and h_ϕ with the known equations for the Polder susceptibility tensor solved from the Landau-Lifshitz-Gilbert (LLG) equation,[18,23,24] one can calculate the time average of $V(t)$ to obtain the dc rectification voltage

$$V_{SR}(H, \theta_M, \phi_M) = \frac{R_S I_1}{2\alpha_{eff}\omega(2H_{eff} + 4\pi M_S \sin^2\theta_M)} \times \left\{ \sin 2\theta_M \sin^2\phi_M \left[\left(A_{\theta\theta} h_\theta^r + A_{\theta\phi} h_\phi^i\right) \mathrm{Sym}(H) + \left(A_{\theta\theta} h_\theta^i - A_{\theta\phi} h_\phi^r\right) \mathrm{Asym}(H) \right] + \sin 2\phi_M \sin\theta_M \left[\left(A_{\phi\theta} h_\theta^i - A_{\phi\phi} h_\phi^r\right) \mathrm{Sym}(H) + \left(A_{\phi\theta} h_\theta^r + A_{\phi\phi} h_\phi^i\right) \mathrm{Asym}(H) \right] \right\}, \quad (2)$$

where $A_{\theta\theta} = \gamma H_{eff}$, $A_{\theta\phi} = A_{\phi\theta} = \omega$, $A_{\phi\phi} = \gamma(H_{eff} + 4\pi M_S \sin^2\theta_M)$, $h_\theta^r = h_\theta \cos\delta$, $h_\theta^i = h_\theta \sin\delta$, $h_\phi^r = h_\phi \cos\delta$, $h_\phi^i = h_\phi \sin\delta$, γ is the gyromagnetic ratio, and α_{eff} is the effective Gilbert damping constant of the YIG/Pt bilayer.[25] The effective field H_{eff} is given by $H_{eff} = |\mathbf{H} - \mathbf{e}_z 4\pi M_S \cos\theta_M|$, where the second term is the demagnetization field along the z-direction. It is clear that V_{SR} has two contributions: one symmetric component and one antisymmetric component with respect to H_r, similar to the AMR-induced SRE.[24]

For the experimental geometry shown in Fig. 2(a), $\mathbf{h}$ is almost along the y-direction. When $\mathbf{H}$ is scanned in the xy-plane, i.e., $\theta_M = \pi/2$, the antisymmetric line shape dc voltage resulting from SMR in Eq. (2) is reduced to

$$V_A^{xy}(H, \phi_M) = V_{SR}^{A,xy} \sin 2\phi_M \cos\phi_M \mathrm{Asym}(H), \quad (3)$$

where $V_{SR}^{A,xy} = \frac{\gamma h I_1 R_S H_{eff}}{2\alpha_{eff}\omega(2H_{eff} + 4\pi M_S)}\cos\delta$. SPE[2] and the SMR-induced SRE lead to a symmetric dc voltage

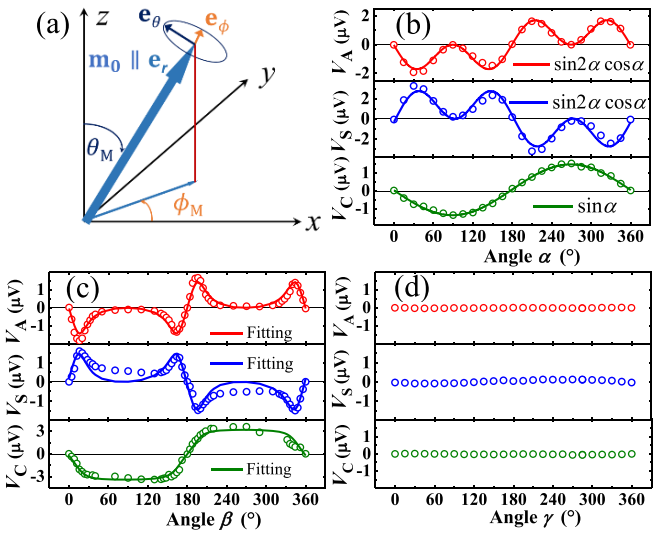

FIG. 3. (a) Spatial coordinates of the precession of $\mathbf{M}$, where $\mathbf{m}_0$ denotes the unit vector in the direction of the equilibrium magnetization. (b)–(d) α, β, and γ dependence of V_A (red circles), V_S (blue circles), and V_C (green circles), respectively. The red and blue solid curves are the fittings to Eqs. (3) and (4) (α-scan) or Eqs. (5) and (6) (β-scan). The green solid curves are the fittings according to the spin Seebeck effect scenario.

$$V_S^{xy}(H, \phi_M) = \left(V_{SR}^{S,xy} + V_{SP}^{xy}\right) \sin 2\phi_M \cos\phi_M \mathrm{Sym}(H), \quad (4)$$

where the first term is reduced from Eq. (2), $V_{SR}^{S,xy} = V_{SR}^{A,xy}\tan\delta$, and the second term is contributed from the SPE with a prefactor of V_{SP}^{xy}.[26] When $\mathbf{H}$ is scanned in the yz-plane, i.e., $\phi_M = \pi/2$, the SRE and SPE give dc voltage

$$V_A^{yz}(H, \theta_M) = V_{SR}^{A,yz} \sin 2\theta_M \cos\theta_M \mathrm{Asym}(H) \quad (5)$$

and

$$V_S^{yz}(H, \theta_M) = (V_{SR}^{S,yz} + V_{SP}^{yz}) \sin 2\theta_M \cos\theta_M \mathrm{Sym}(H), \quad (6)$$

respectively, where $V_{SR}^{A(\mathrm{or}\,S),yz} = \frac{\gamma h I_1 R_S H_{eff}}{2\alpha_{eff}\omega\left(2H_{eff} + 4\pi M_S \sin^2\theta_M\right)}\cos\delta$ (or $\sin\delta$) and V_{SP}^{yz} is a parameter to indicate the contribution of the SPE. For $\mathbf{H}$ in the xz-plane, i.e., $\phi_M = 0$, the SRE vanishes according to Eq. (2) due to the absence of SMR in this experimental geometry [bottom panel of Fig. 1(c)]. In

contrast, in this geometry, the AMR-induced SRE is non-zero. Therefore, the measurement in this geometry is a simple and crucial approach to distinguish the SMR- and AMR- induced SRE.[9,27,28]

Then, we tested the theoretical model with experiments. Figures 3(b)–3(d) show the angle α, β and, γ dependence of V_S, V_A, and V_C, which are obtained by fitting $V(H)$ in each spectrum, with **H** scanning within *xy*-, *yz*-, and *xz*-planes, respectively. For **H** in the *xy*-plane, H_r is much larger than the in-plane anisotropy field. **M** is fully aligned with **H**, i.e., $\phi_M = \alpha$. V_C presents a sinα dependence [bottom panel of Fig. 3(b)]. For **H** in the *yz*-plane, H_r is not strong enough to align **M** with **H** due to the demagnetization field, i.e., $\theta_M \neq \beta$. We took the demagnetization field into account to calculate θ_M for each H_r. H_r is about 500 Oe for **H** in the sample plane. H_r is about 2800 Oe for **H** along the *z*-direction, which is larger than the saturation field of about 1800 Oe. We found that V_C follows a sinθ_M function very well [bottom panel of Fig. 3(c) and the supplementary material]. For **H** in the *xz*-plane, V_C disappears [bottom panel of Fig. 3(d)]. These behaviors of V_C can be explained by the scenario of the combined processes of the longitudinal spin Seebeck effect and ISHE.[29,30] The temperature gradient in Pt/YIG arises from the microwave heating, as in previous reports.[31,32]

Utilizing Eqs. (3)–(6), we fitted the data for **H** in *xy*- and *yz*-planes [top and middle panels of Figs. 3(b) and 3(c)]. The fittings reproduce the data well, strongly suggesting that the asymmetric component solely originates from the SMR-induced SRE. For **H** in the *xz*-plane, we did not observe the dc voltage [top and middle panels of Fig. 3(c)], as expected from the theoretical analysis. These results demonstrate that the observed signal is the SMR-induced SRE.

From Eqs. (4) and (6), we learned that both the SPE and the SRE present $\sin 2\phi_M \cos\phi_M$ or $\sin 2\theta_M \cos\theta_M$ dependence for the symmetric component when **H** is in the *xy*- or *yz*-plane. The relative contribution to the electromotive force of these two effects cannot be quantitatively separated. To further study the SMR-induced SRE, we changed the experimental geometry by applying **h** along the *x*-direction. To achieve this, we put a short sample in the center of the CPW and $V(H)$ is measured perpendicular to the CPW signal line (*x*-direction),[33] as shown in Fig. 4(a). The optical images of the device are in the supplementary material. Figure 4(b) shows the angle α dependence of V_S and V_A extracted from the $V(H)$ spectrum with **H** scanning within the *xy*-plane. In this experimental geometry, the SRE and the SPE give two dc voltage components

$$V_A^{xy}(H,\phi_M) = V_{SR}^{A,xy}\sin 2\phi_M \sin\phi_M \mathrm{Asym}(H) \quad (7)$$

and

$$V_S^{xy}(H,\phi_M) = \left(V_{SR}^{S,xy}\sin 2\phi_M \sin\phi_M + V_{SP}^{xy}\sin\phi_M \sin^2\phi_M\right)\mathrm{Sym}(H), \quad (8)$$

respectively. Indeed, the angular dependence can be well fitted by Eqs. (7) and (8), as shown in Fig. 4(b). The rf current in Pt might induce the magnetization precession of YIG via the spin-torque FMR effect, which can lead to the SRE. The angular dependence of the spin-torque FMR-induced SRE

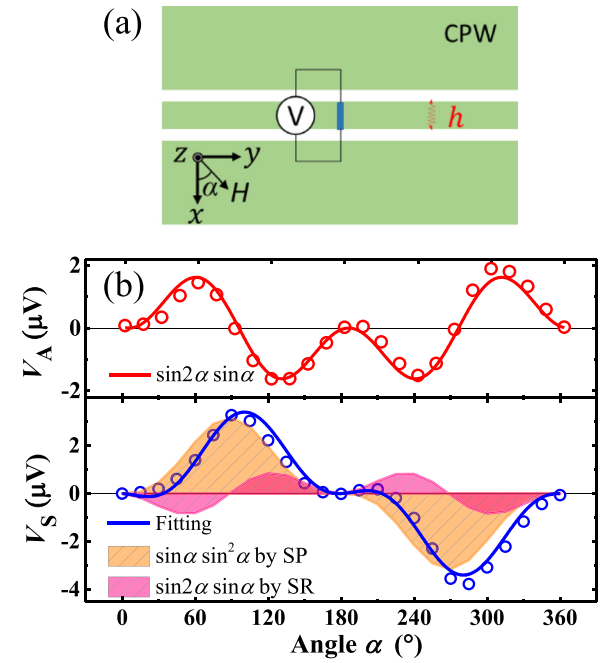

FIG. 4. (a) Sketch of the experimental set-up. A short sample was placed in the center of the CPW with **h** mainly along the *x*-axis. (b) V_A (red circles) and V_S (blue circles) as a function of α. The red solid curve is the fitting according to Eq. (7). The blue curve is the fitting according to Eq. (8). The dc voltage is the superposition of SPE (yellow) and SRE (pink) components.

presents $\sin 2\phi_M \cos\phi_M$ dependence for **H** in the *xy*-plane.[34] However, the SRE voltage follows $\sin 2\phi_M \sin\phi_M$ behavior well [Fig. 4(b)], meaning that the spin-torque FMR effect is negligible. Again, these results unambiguously confirm that the SMR effect can induce the SRE in Pt/YIG. The fittings yield $V_{SR}^{A,xy} = 2.10\mu$V, $V_{SR}^{S,xy} = -1.11\mu$V, and $V_{SP}^{xy} = 3.16\mu$V. The contributions of the SPE and SRE are comparable. Although, the MR ratio of our sample is only about 0.028% [Fig. 1(c)], the absolute resistance change R_S is about 0.7 Ω for our very thin Pt film. α_{eff} of the YIG/Pt bilayer is about 4.54×10^{-3} (see supplementary material). With other parameters: $4\pi M_S = 1750$ Oe, $\gamma = 1.76 \times 10^{11}\mathrm{T}^{-1}\mathrm{s}^{-1}$, $f = 3$ GHz, and $H_{eff} = 502$ Oe, we obtained $hI_1 \approx 11.55\,\mathrm{mA}\cdot\mu\mathrm{T}$, which is a reasonable value for the CPW with a power of 100 mW.[24] We note that the large R_S and low α_{eff} are critical to the observation of the SMR-induced SRE.

In conclusion, we experimentally demonstrated that the SMR effect can induce a spin rectification effect in the Pt/YIG bilayer under FMR. Our conclusion is fully supported by three evidences: (1) An asymmetric dc voltage with respect to the magnetic resonance field is observed. (2) The dc voltage as functions of the magnetic field directions can be well-fitted by the model based on the SMR-induced spin rectification when the field is applied in *xy*- and *yz*-planes. (3) Both SMR and the dc voltage vanish when the field is applied in the *xz*-plane. Furthermore, we found that the SMR-induced spin rectification effect can be quantitatively separated from the spin pumping effect when the microwave magnetic field is applied along the measurement direction.

See supplementary material for the characterization of YIG, SMR in β-scan, sample images, angular dependence of V_A, V_S, and V_C for magnetic field in *yz*-plane, the

effective Gilbert damping constant of YIG/Pt bilayer, and MR at large field.

This work was supported by the National Basic Research Program of China (Grant No. 2013CB922103), the NSF of China (Grant Nos. 11674159, 51471086, and 11222435), and the NSF of Jiangsu Province (Grant No. BK20130054).

[1]A. Hoffmann, IEEE. Trans. Magn. **49**, 5172 (2013).
[2]E. Saitoh, M. Ueda, H. Miyajima, and G. Tatara, Appl. Phys. Lett. **88**, 182509 (2006).
[3]K. Ando, S. Takahashi, J. Ieda, Y. Kajiwara, H. Nakayama, T. Yoshino, K. Harii, Y. Fujikawa, M. Matsuo, S. Maekawa, and E. Saitoh, J. Appl. Phys. **109**, 103913 (2011).
[4]Y. S. Gui, N. Mecking, X. Zhou, G. Williams, and C.-M. Hu, Phys. Rev. Lett. **98**, 107602 (2007).
[5]H. Chen, X. Fan, H. Zhou, W. Wang, Y. S. Gui, C.-M. Hu, and D. Xue, J. Appl. Phys. **113**, 17C732 (2013).
[6]A. Yamaguchi, K. Motoi, A. Hirohata, and H. Miyajima, Phys. Rev. B **79**, 224409 (2009).
[7]M. Harder, Y. Gui, and C.-M. Hu, e-print arXiv:1605.00710.
[8]A. Azevedo, L. H. Vilela-Leão, R. L. Rodríguez-Suárez, A. F. Lacerda Santos, and S. M. Rezende, Phys. Rev. B **83**, 144402 (2011).
[9]L. Bai, P. Hyde, Y. S. Gui, C.-M. Hu, V. Vlaminck, J. E. Pearson, S. D. Bader, and A. Hoffmann, Phys. Rev. Lett. **111**, 217602 (2013).
[10]L. Bai, Z. Feng, P. Hyde, H. F. Ding, and C.-M. Hu, Appl. Phys. Lett. **102**, 242402 (2013).
[11]B. Heinrich, C. Burrowes, E. Montoya, B. Kardasz, E. Girt, Y.-Y. Song, Y. Sun, and M. Wu, Phys. Rev. Lett. **107**, 066604 (2011).
[12]C. Hahn, G. de Loubens, O. Klein, M. Viret, V. V. Naletov, and J. Ben Youssef, Phys. Rev. B **87**, 174417 (2013).
[13]H. Nakayama, M. Althammer, Y.-T. Chen, K. Uchida, Y. Kajiwara, D. Kikuchi, T. Ohtani, S. Geprägs, M. Opel, S. Takahashi, R. Gross, G. E. W. Bauer, S. T. B. Goennenwein, and E. Saitoh, Phys. Rev. Lett. **110**, 206601 (2013).
[14]Y.-T. Chen, S. Takahashi, H. Nakayama, M. Althammer, S. Goennenwein, E. Saitoh, and G. Bauer, Phys. Rev. B **87**, 144411 (2013).
[15]Y. M. Lu, J. W. Cai, S. Y. Huang, D. Qu, B. F. Miao, and C. L. Chien, Phys. Rev. B **87**, 220409(R) (2013).
[16]M. Althammer, S. Meyer, H. Nakayama, M. Schreier, S. Altmannshofer, M. Weiler, H. Huebl, S. Geprägs, M. Opel, R. Gross, D. Meier, C. Klewe, T. Kuschel, J.-M. Schmalhorst, G. Reiss, L. Shen, A. Gupta, Y.-T. Chen, G. E. W. Bauer, E. Saitoh, and S. T. B. Goennenwein, Phys. Rev. B **87**, 224401 (2013).
[17]M. Isasa, A. Bedoya-Pinto, S. Vélez, F. Golmar, F. Sánchez, L. E. Hueso, J. Fontcuberta, and F. Casanova, Appl. Phys. Lett. **105**, 142402 (2014).
[18]R. Iguchi, K. Sato, D. Hirobe, S. Daimon, and E. Saitoh, Appl. Phys. Express **7**, 13003 (2014).
[19]J. Rao, X. Fan, L. Ma, H. Zhou, X. Zhao, J. Zhao, F. Zhang, S. Zhou, and D. Xue, J. Appl. Phys. **117**, 17C725 (2015).
[20]B. F. Miao, S. Y. Huang, D. Qu, and C. L. Chien, Phys. Rev. Lett. **112**, 236601 (2014).
[21]S. Vélez, V. N. Golovach, A. Bedoya-Pinto, M. Isasa, E. Sagasta, M. Abadia, C. Rogero, L. E. Hueso, F. S. Bergeret, and F. Casanova, Phys. Rev. Lett. **116**, 016603 (2016).
[22]O. Mosendz, J. E. Pearson, F. Y. Fradin, G. E. W. Bauer, S. D. Bader, and A. Hoffmann, Phys. Rev. Lett. **104**, 046601 (2010).
[23]A. G. Gurevich and G. A. Melkov, Magnetization Oscillations and Waves (CRC Press, Boca Raton, Florida, 1996).
[24]N. Mecking, Y. S. Gui, and C.-M. Hu, Phys. Rev. B **76**, 224430 (2007).
[25]Y. Sun, H. Chang, M. Kabatek, Y.-Y. Song, Z. Wang, M. Jantz, W. Schneider, M. Wu, E. Montoya, B. Kardasz, B. Heinrich, S. G. E. te Velthuis, H. Schultheiss, and A. Hoffmann, Phys. Rev. Lett. **111**, 106601 (2013).
[26]O. Mosendz, V. Vlaminck, J. E. Pearson, F. Y. Fradin, G. E. W. Bauer, S. D. Bader, and A. Hoffmann, Phys. Rev. B **82**, 214403 (2010).
[27]M. Harder, Z. X. Cao, Y. S. Gui, X. L. Fan, and C.-M. Hu, Phys. Rev. B **84**, 054423 (2011).
[28]T. Chiba, M. Schreier, G. E. W. Bauer, and S. Takahashi, J. Appl. Phys. **117**, 17C715 (2015).
[29]K. Uchida, H. Adachi, T. Ota, H. Nakayama, S. Maekawa, and E. Saitoh, Appl. Phys. Lett. **97**, 172505 (2010).
[30]T. Kikkawa, K. Uchida, Y. Shiomi, Z. Qiu, D. Hou, D. Tian, H. Nakayama, X.-F. Jin, and E. Saitoh, Phys. Rev. Lett. **110**, 067207 (2013).
[31]M. Agrawal, A. A. Serga, V. Lauer, E. T. Papaioannou, B. Hillebrands, and V. I. Vasyuchka, Appl. Phys. Lett. **105**, 092404 (2014).
[32]N. Roschewsky, M. Schreier, A. Kamra, F. Schade, K. Ganzhorn, S. Meyer, H. Huebl, S. Geprägs, R. Gross, and S. T. B. Goennenwein, Appl. Phys. Lett. **104**, 202410 (2014).
[33]S. W. Jiang, S. Liu, P. Wang, Z. Z. Luan, X. D. Tao, H. F. Ding, and D. Wu, Phys. Rev. Lett. **115**, 086601 (2015).
[34]T. Chiba, G. E. W. Bauer, and S. Takahashi, Phys. Rev. Appl. **2**, 034003 (2014).